Dentomaxillofacial Radiology (2018) 47, 20170343

birpublications.org/dmfr

RESEARCH ARTICLE

Characterization of salivary gland tumours with diffusion tensor imaging

Ahmed Abdel Khalek Abdel Razek

Department of Diagnostic Radiology, Mansoura Faculty of medicine, Mansoura, Egypt

Objectives: To characterize salivary glands tumours with diffusion tensor imaging.
Methods: This study was conducted upon 53 patients (aged 18–81 years: mean 37 years) with salivary gland tumours that underwent diffusion tensor imaging was obtained using a single-shot echoplanar imaging sequence with parallel imaging at 1.5 T scanner. 48 slices were obtained, with a thickness of 2.5 mm, with no gap and the total scan duration was 7–8 min. The fractional anisotropy (FA) and the mean diffusivity (MD) value of the salivary gland tumours was calculated and correlated with pathological findings. Image analysis was performed by one radiologist. The receiver operating characteristic curve was drawn to detect the cut-off point of FA and MD used to characterize salivary gland tumours.
Results: The mean FA and MD of malignant salivary gland tumours (n = 17) (0.41 ± 0.07 and $0.89 \pm 0.15 \times 10^{-3}$ mm^2 s^{-1}) was significantly different ($p = 0.001$) than that of benign tumours (n = 36) (0.19 ± 0.07 and $1.28 \pm 0.42 \times 10^{-3}$ mm^2 s^{-1}), respectively. Combined FA and MD used to differentiate malignant from benign tumours has an area under the curve (AUC) of 0.974, and an accuracy of 86%. There was a significant difference in FA between Warthin tumours and malignant tumours ($p = 0.001$). Selection FA of 0.35 to differentiate malignant tumours from Warthin tumours revealed AUC of 0.878 and an accuracy of 80%. There was a significant difference in FA and MD of malignant tumours and pleomorphic adenomas ($p = 0.001$). Combined FA and MD used to differentiate malignant tumours from pleomorphic adenomas revealed AUC of 0.993, and an accuracy of 93%. There was a significant difference in FA and MD of Warthin tumours and pleomorphic adenomas (p = 0.001). Combined FA and MD used to differentiate Warthin tumours from pleomorphic adenomas revealed AUC of 0.978, and an accuracy of 86%.
Conclusions: Diffusion-weighed imaging is a promising non-invasive method and it may be useful for the characterization and differentiation of benign and malignant salivary gland tumours.
Dentomaxillofacial Radiology (2018) **47**, 20170343. doi: 10.1259/dmfr.20170343

Cite this article as: Khalek Abdel Razek A A. Characterization of salivary gland tumours with diffusion tensor imaging. *Dentomaxillofac Radiol* 2018; **47**: 20170343.

Keywords: diffusion tensor imaging; salivary; tumors

Introduction

Salivary gland tumours are rare with an overall incidence of 2.5–3.0 cases per 100,000 per year. Malignant salivary gland tumours account for more than 0.5% of all malignancies and approximately, 3 to 5% of all head and neck cancers.[1,2] Characterization of salivary gland tumours is important for pre-operative treatment planning. The surgery chosen for treatment of salivary gland tumours depends on the histologic type of the tumour. Superficial parotidectomy is done for benign tumours and total parotidectomy with radiotherapy was preferred for malignant tumours.[2–5] Ultrasound and CT have limited role in the characterization of salivary tumours.[6–11] Morphological imaging findings at routine CT and MRI cannot differentiate malignant

Correspondence to: Prof Ahmed Abdel Khalek Abdel Razek, E-mail: arazek@mans.edu.eg

Received 07 September 2017; revised 31 January 2018; accepted 05 February 2018

from benign salivary tumours.[9–12] Diffusion-weighted MRI alone or combined with perfusion-weighted MRI is used for characterization of salivary gland tumours with varies results along different authors.[13–19]

Diffusion-weighted MRI depicts the Brownian motion of water molecules in biological tissues. Different studies discuss the role of diffusion-weighted MRI in evaluation of brain tumours and infection. The apparent diffusion coefficient (ADC) is a parameter of diffusion-weighted MRI that can differentiate malignant head and neck tumours from benign lesions and infection, grading of malignancy and prediction of treatment response. Malignant tumours show restricted diffusion with low ADC value and benign tumours show unrestricted diffusion with high ADC value.[20–22] Diffusion tensor imaging is an emerging MRI technique which reflects micromovement of water molecules and can distinguish between different tissue compartments at the cellular level with different matrices. The most common metrics of diffusion tensor imaging used are fractional anisotropy (FA) and mean diffusivity (MD).[23] Few studies discuss role of diffusion tensor imaging of parotid tumours and head and neck have been reported.[24–26]

The aim of this work was to characterize salivary gland tumours with diffusion tensor imaging.

Methods and materials

Patients

Institutional review board approval was obtained and informed consent was waived because this is a retrospective study. A retrospective analysis was performed on 55 consecutive patients with salivary gland tumours. Inclusion criteria were patients with salivary gland tumours that underwent diffusion tensor imaging. Two patients were excluded from the study due to motion artefacts. The final patients included in this study were 53 patients (28 male and 25 female, age ranged from 18–81 years; mean age 37 years). The final diagnosis was done by histopathological examination in all cases with surgical biopsy (n = 27), fine needle aspiration biopsy (n = 9) and core biopsy (n = 7). The tumour was located in the parotid gland in 43 patients and submandibular gland in 10 patients. Multiple lesions were seen in seven patients with Warthin tumours. The biopsy was done after MRI. All patients underwent routine pre- and post-contrast MRI and diffusion tensor imaging of parotid gland before biopsy or surgery. The pathological diagnosis of the malignant salivary gland tumours (n = 17) were mucoepidermoid carcinoma (n = 6), adenoid cystic carcinoma (n = 6), carcinoma exadenoma (n = 2), lymphoepithelial carcinoma metastasis (n = 2) and squamous cell carcinoma adenoid cystic carcinoma (n = 1). The benign salivary tumours (n = 36) were Warthin tumour (n = 14), pleomorphic adenoma (n = 18), basal cell adenomas (n = 2), and monomorphic adenomas (n = 2).

MRI

All MR images were acquired on a 1.5 T scanner (Ingenia, Philips, Philips Medical Systems, Best, Netherlands). The machine equipped with a self-shielding gradient set (30 mTm maximum gradient strength, 120 T m^{-1} s^{-1} slew rate) and) with a 16-channel neurovascular coil. All patients underwent T_1 weighted images [repetition time (TR)/echo time (TE) = 800/15 ms) and T_2 weighted fast spin echo images (TR/TE = 6000/80 ms). The scanning parameters were section thickness = 5 mm, an interslice gap = 1.5 mm, a field of view (FOV) = 25–30 cm and an acquisition matrix = 256 × 224. Routine post-contrast study T_1 weighted images were obtained after intravenous administration of gadoterate meglumine, 0.2 ml kg^{-1} (0.1 mmol kg^{-1}) body weight using 20–22 G venous cannula with a flow rate of 2 ml s^{-1}. The scanning parameters were TR/TE = 800/15 ms, section thickness = 5 mm, an interslice gap = 1.5 mm, FOV = 25–30 cm and an acquisition matrix = 256 × 224.

Diffusion tensor imaging

Diffusion tensor imaging was obtained using a Single-shot echo planar imaging sequence (TR/TE = 3200/90 ms) with parallel imaging [SENSitivity Encoding (SENSE) reduction factor P 2]. Automatic multiangle-projection shim and chemical shift selective fat suppression technique applied to reduce the artefacts at diffusion-weighted MR images. Diffusion gradients were applied along 32 axes, using a b-value of 0 and 1000 s mm^{-2}. The scanning parameters were: FOV = 250 × 170 mm^2, data matrix = 92 × 88 and voxel dimensions = 2.43 × 2.54 × 2.5 mm^3. 48 slices were obtained, with a thickness of 2.5 mm, with no gap and the total scan duration was 7–8 min. Diffusion tensor imaging was performed in an axial section before contrast medium injection.

Image analysis

Image analysis was performed by one radiologist (AA) expert in head and neck radiology, since 25 years that was blinded to the clinical presentation and final pathological results. The images were transferred to the workstation (extended MR Workspace 2.6.3.5, Philips medical systems, Best, Netherlands). The images were loaded to diffusion tensor imaging software workstation (View Forum 7.2.0.1 exported patient image data, Philips medical system, Best, Netherlands). Automated registration of the diffusion tensor imaging data was done to eliminate eddy current artefacts. Co-registration of the FA maps to contrast T_1 weighted images was done for accurate placement of region of interest. In patients with multiple focal lesions, the largest lesion was selected for analysis. A round region of interest was placed at co-registered FA map to contrast T_1 weighted image around the enhanced region of the tumour using an electronic cursor. The FA and MD were calculated according to previously described equation.[23–25]

Table 1 Mean, standard deviation, minimum, maximum, of FA and MD (10^{-3}mm^2 s^{-1}) of malignant and benign salivary gland tumours

Pathology	*FA*	*MD (10^{-3} mm^2 s^{-1})*
Malignant (n = 7)	0.41 ± 0.07 (0.26–0.51)	0.89 ± 0.15 (0.75–1.27)
Mucoepider carcinoma (n = 6)	0.46 ± 0.03 (0.26–0.51)	0.89 ± 0.19 (0.75–1.27)
Adenoid cystic carcinoma (n = 6)	0.38 ± 0.08 (0.26–0.48)	0.87 ± 0.07 (0.77–0.94)
Ca expleomorphic adenoma (n = 2)	0.36 ± 0.11 (0.28–0.44)	0.83 ± 0.08 (0.77–0.88)
Lymphoepithelial carcinoma (n = 2)	0.42 ± 0.08 (0.37–0.48)	0.92 ± 0.20 (0.77–1.07)
Squamous cell carcinoma (n = 1)	0.44	1.15
Benign (n = 36)	0.19 ± 0.07 (0.11–0.39)	1.28 ± 0.42 (0.68–1.81)
Pleomorphic adenomas (n = 18)	0.15 ± 0.03 (0.11–0.23)	1.61 ± 0.18 (1.23–1.8)
Warthin tumours (n = 14)	0.25 ± 0.07 (0.17–0.39)	0.79 ± 0.06 (0.68–0.89)
Basal cell adenomas (n = 2)	0.12 ± 0.02 (0.11–0.14)	1.61 ± 0.02 (1.59–1.62)
Monomorphic adenomas (n = 2)	0.15 ± 0.01 (0.15–0.16)	1.55 ± 0.04 (1.52–1.58)
p-value	$p = 0.001$	$p = 0.0001$

FA, fractional anisotropy; MD, mean diffusivity.

Statistical analysis

The statistical analysis of data was done by using Statistical Package for Social Science v. 21 (SPSS Inc., Chicago, IL). The mean and standard deviation of FA and MD value of malignant and benign parotid tumours were calculated. The analysis of data was done to test the statistically significant difference. Student's *t*-test was used to compare between the FA and MD of malignant and benign salivary tumours. A *p*-value less than 0.05 was considered statistically significant. The receiver operating characteristic curve was drawn. The cut-off point of FA and MD value with highest accuracy was selected to differentiate malignant from benign tumours, Warthin tumours from malignant tumours and Warthin tumours from pleomorphic adenoma with the calculation of the AUC, accuracy, sensitivity, and specificity. Multivariate analysis was performed for combined FA and MD with statistically significant *p*-value (<0.05) with creation of the receiver operating characteristic curve to detect best accuracy with calculation of AUC, sensitivity and specificity.

Results

Table 1 shows the mean, standard deviation, minimum and maximum of FA and MD of malignant and benign salivary glands tumours. Table 2 shows the results of receiver characteristic curve with cut-off values of FA and MD of malignant and benign parotid tumours.

The mean FA and MD of malignant salivary gland tumours (Figure 1) (0.41 ± 0.07 and 0.89 ± 0.15 × 10^{-3} mm^2 s^{-1}) was significant difference ($p = 0.001$) than benign salivary gland tumours (Figures 2 and 3) (0.19 ± 0.07 and 1.28 ± 0.42 × 10^{-3} mm^2 s^{-1}), respectively. Selection FA of 0.27 and MD of 1.19 × 10^{-3} mm^2 s^{-1}

Table 2 Results of ROC curve with calculation of AUC, accuracy, sensitivity, and specificity of FA and MD (10^{-3}mm^2 s^{-1}) malignant and benign salivary gland tumours

Parameter	*Cut-of point*	*AUC*	*Accuracy*	*Sensitivity*	*Specificity*
Malignant *vs* benign					
FA	0.27	0.975	86	88	86
MD (10^{-3} mm^2 s^{-1})	1.19	0.708	69	94	85
Combined FA and MD		0.974	86	100	80
Malignant *vs* Warthin					
FA	0.35	0.878	80	85	76
Malignant *vs* Pleomorphic					
FA	0.22	0.884	94	94	93
MD (10^{-3} mm^2 s^{-1})	1.25	0.996	91	94	93
Combined FA and MD		0.993	93	94	94
Warthin *vs* Pleomorphic					
FA	0.17	0.971	83	93	81
MD (10^{-3} mm^2 s^{-1})	1.06	0.897	93	94	93
Combined FA and MD		0.978	86	92	81

AUC, area under the curve; FA, fractional anisotropy; MD, mean diffusivity.

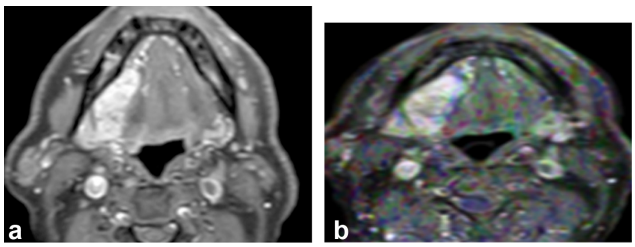

Figure 1 *Mucoepidermoid carcinoma of the submandibular gland.* (a) Axial contrast *T*1 weighted MR image shows inhomogeneous enhancement of the tumour. (b) Colour FA map co-registered with contrast *T*1 weighted image shows the tumour with high FA (0.43) and low MD value (0.88×10^{-3} mm^2 s^{-1}). FA, fractional anisotropy; MD, mean diffusivity.

to differentiate malignant from benign salivary gland tumours revealed an area under the curve (AUC) of 0.975, 0.708 and accuracy of 86, 69%, a sensitivity of 88 and 94% and specificity of 85 and 80%, respectively. Combined FA and MD used to differentiate malignant from benign salivary gland tumours has an AUC of 0.974, an accuracy of 86%, a sensitivity of 100% and specificity of 80% (Figure 4).

The mean FA of Warthin tumours (Figure 2) (0.25 ± 0.07) was a significant difference ($p = 0.001$) than that of malignant tumours (0.41 ± 0.07). There was insignificant difference in the MD ($p = 0.02$) between Warthin tumours ($0.79 \pm 0.06 \times 10^{-3}$ mm^2 s^{-1}) and malignant salivary gland tumours ($0.89 \pm 0.15 \times 10^{-3}$ mm^2 s^{-1}). Selection of FA of 0.35 to differentiate Warthin tumours from malignant salivary gland tumours revealed an AUC of 0.878, an accuracy of 80% sensitivity of 85% and specificity of 76% (Figure 4).

The mean FA and MD of pleomorphic adenoma (0.15 ± 0.03 and $1.61 \pm 0.18 \times 10^{-3}$ mm^2 s^{-1}) was significant difference ($p = 0.001$) than malignant tumours (0.41 ± 0.07 and $0.89 \pm 0.15 \times 10^{-3}$ mm^2 s^{-1}), respectively. Selection of FA of 0.22 and MD of 1.25×10^{-3} mm^2 s^{-1} to differentiate pleomorphic adenoma from malignant tumours revealed AUC of 0.884, 0.996 and accuracy of 94, 94%, a sensitivity of 94, 94% and specificity of 93 and 93%, respectively. Combined FA and MD used to differentiate pleomorphic adenomas from malignant tumours has an AUC of 0.993, an accuracy of 93%, a sensitivity of 94% and specificity of 94% (Figure 4).

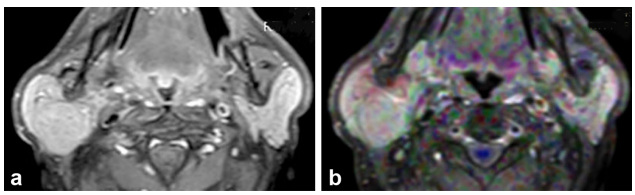

Figure 2 *Warthin tumour of the right parotid.* (a) Axial contrast *T*1 weighted MR image shows homogeneous enhancement of the tumour. (b) Colour FA map shows the tumour with low FA (0.23) and low MD value (0.72×10^{-3} mm^2 s^{-1}). FA, fractional anisotropy; MD, mean diffusivity.

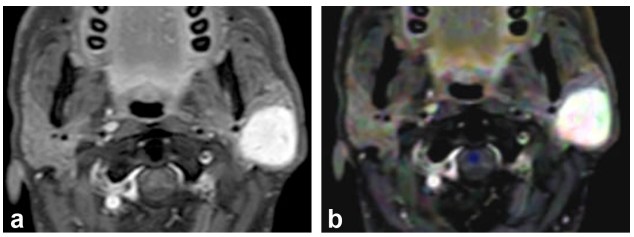

Figure 3 *Pleomorphic adenoma of the right parotid.* (a) Axial contrast *T*1 weighted MR image shows homogeneous enhancement of the tumour. (b) Colour FA map shows the tumour with low FA (0.14) and high MD value (1.59×10^{-3} mm^2 s^{-1}). FA, fractional anisotropy; MD, mean diffusivity.

The mean FA and MD of pleomorphic adenoma (Figure 3) (0.15 ± 0.03 and $1.61 \pm 0.18 \times 10^{-3}$ mm^2 s^{-1}) was significant difference ($p = 0.001$) than Warthin tumours (0.25 ± 0.07 and $0.79 \pm 0.06 \times 10^{-3}$ mm^2 s^{-1}), respectively. Selection FA of 0.17 and MD of 1.06×10^{-3} mm^2 s^{-1} to differentiate pleomorphic adenoma from Warthin tumours revealed AUC of 0.971, 0.897 and accuracy of 83, 93%, a sensitivity of 93 and 94%, and specificity of 81 and 93%, respectively. Combined FA and MD used to differentiate Warthin tumours from pleomorphic adenomas has an AUC of 0.978, an accuracy of 86%, a sensitivity of 92% and specificity of 81% (Figure 4).

Discussion

The main findings of this study are diffusion tensor imaging can use for characterization of salivary tumours. Combined FA and MD can differentiate malignant from benign salivary gland tumours and Warthin tumours from pleomorphic adenomas and FA only can differentiate Warthin tumours from malignant salivary gland tumours.

The most common metrics of DTI used are MD and FA. The MD is the average diffusivity along three orthogonal planes in x,y,z directions of the tensor, which is equal to the average of the three eigenvalues and equivalent to ADC value. The MD reveals the rate of water molecules' diffusional motion as the tumour cellularity is the main target of histologic tumour classification with DTI. There is an inverse relationship between the cellularity of the tumour and the MD value.[27–29] One study reported that the FA predominantly represents the degree of the directionality of water diffusion of the tissue microstructure and related to the structural orientation of the different tissues. The FA value range is 0–1. FA values equal 0 for the isotropic condition, in which diffusion is equal in all directions, and FA values approach a value of 1 for extreme directional inequality. There is a linear increase in the FA with tumour cellularity and malignancy grade.[27–29]

In this study, there is significant difference in FA and MD of malignant and benign salivary gland tumours ($p = 0.001$) and combined FA and MD are accurate

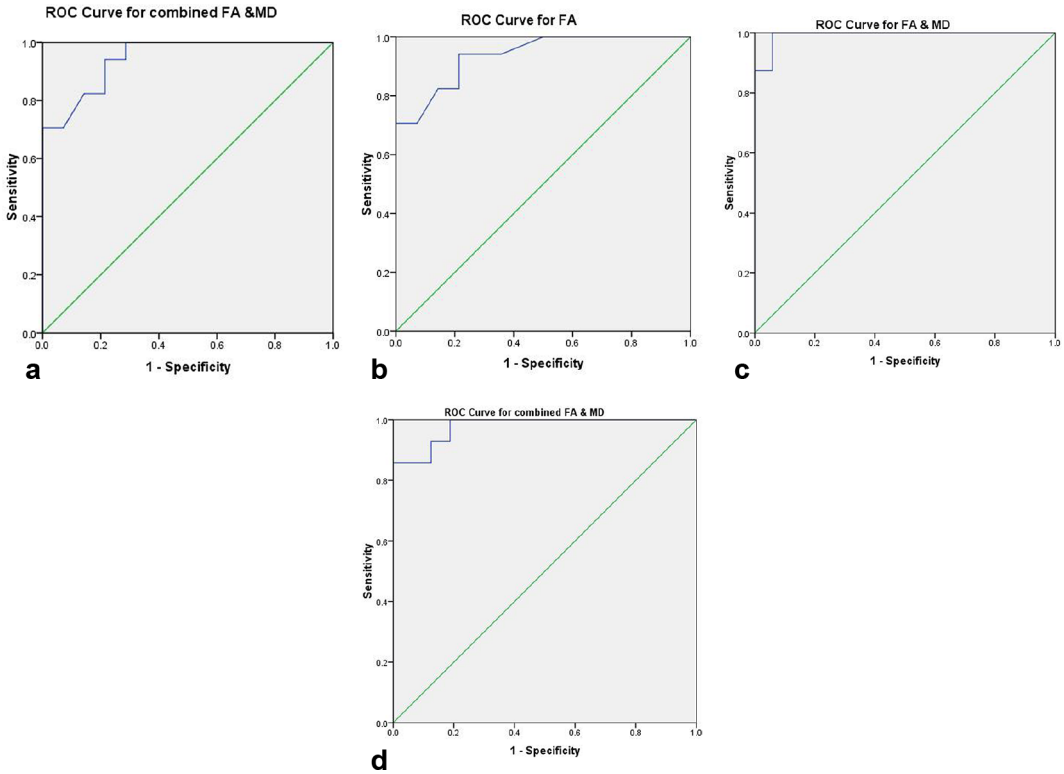

Figure 4 *Receiver operating characteristic curve of FA and MD.* (a) The combined FA and MD used to differentiate malignant from benign salivary gland tumours have under the curve of 0.974 and an accuracy of 86%. (b) The threshold of FA used to differentiate malignant salivary gland tumours from Warthin tumours is 0.35 with an area under the curve of 0.878 and accuracy of 80%. (c) The combined FA and MD used to differentiate malignant salivary gland tumours from pleomorphic adenomas have under the curve of 0.993, and an accuracy of 93%. (d) The combined FA and MD used to differentiate malignant salivary gland tumours from pleomorphic adenomas have under the curve of 0.978, and an accuracy of 86%. FA, fractional anisotropy; MD, mean diffusivity.

parameters for differentiating malignant from benign salivary gland tumours. One study reported that there is a significant difference in the ADC and FA of diffusion tensor imaging (p = 0.032, p = 0.011) between benign and malignant parotid tumours. The cut-off ADC and FA used to differentiate benign and malignant salivary gland tumours are 1.02 × 10^{-3} mm^2 s^{-1} and 0.24, with sensitivity of 87.50, 62.50, respectively.[26] Another study added that there is insignificant difference in ADC (p = 0.225) and significant higher FA of malignant parotid tumours compared to benign tumours (0.26 ± 0.06 *vs* 0.17 ± 0.05). The AUC of FA used to predict malignant parotid tumours is greater than that the AUC of ADC (0.884 *vs* 0.628).[24] Another study reported that diffusion tensor imaging is a useful predictor of malignancy for head and neck tumours, with ADC of malignant tumours significantly lower than those of benign lesions.[25] The FA is an indicator for evaluating anisotropic sensitivity. There is positive correlation of the FA value with tumour cellularity, *i.e.* higher FA, is associated with higher tumour cellularity. The FA increased in the abnormal cytoarchitecture of malignancy, which contain variable admixtures of necrosis, disordered hypervascular flow and invaded soft tissue.[26]

In this study, FA is a new marker that helps to differentiate Warthin tumours from other malignant salivary gland tumours. Previous studies reported there is overlap in the ADC and MD value between Warthin tumours and malignant parotid tumours and routine diffusion-weighted MRI cannot differentiate between them.[13,26] Warthin tumours show lower FA than other malignant salivary gland tumours. This may be attributed to less cellularity of Warthin tumours compared to malignant salivary gland tumours that show high cellularity with higher FA.

In this study, diffusion tensor imaging can differentiate malignant tumours from pleomorphic adenomas. One study reported that parotid malignancies have significantly lower ADC and T_{peak}, as well as significantly higher T_{max} and washout rate. An ADC ≤1.267 × 10^3 mm s^{-2} yield optimum accuracy in detection of salivary malignancy with 95.8% sensitivity and 93% specificity.[30] Another study added that there is a significant difference in the ADC and FA between pleomorphic adenoma and malignant tumour (p = 0.0012, p = 0.001).[26]

In this study, the MD alone or combined with FA can differentiate Warthin tumours from pleomorphic adenoma with optimum accuracy. Differentiation Warthin tumours from pleomorphic adenoma is

important due to different prognosis and pattern of management. Previous studies reported that pleomorphic adenoma reveal unrestricted diffusion with higher ADC value compared to Warthin tumours that reveal restricted diffusion. This is attributed to the proliferation of follicle-containing lymphoid tissue in connective tissue of Warthin tumours and myxoid or chondroid texture of the stroma in patients with pleomorphic adenomas.[31,32] Warthin tumours show the highest FA among all benign salivary gland tumours. This may be attributed to presence of excess lymphoid tissue within Warthin tumours with higher anisotropy compared to other benign salivary gland tumours.

In this study, combination of FA and MD increased accuracy of diffusion tensor imaging in characterization of salivary gland tumours. Previous study reported that applied combined 14 diffusion-weighted imaging parameters using monoexponential, biexponential, and triexponential models, stretched exponential model and diffusion kurtosis imaging models to determine head and neck squamous cell carcinoma patients' detailed tissue structures.[33] Another study combined DTI parameters with arterial spin labelling parameter increased accuracy of MRI in differentiation of recurrent gliomas from post-treatment changes.[27] Adding perfusion MRI to the combination of contrast T_1 weighted imaging and diffusion-weighted imaging significantly improves the prediction of recurrent glioblastoma.[34]

There are few limitations of this study. First, the patient populations studied is a small number of patients. Further multicentre studies upon a large number of patients will improve the results. Second, this study used only diffusion tensor imaging, multiparametric MRI of diffusion kurtosis imaging, intravoxel incoherent motion diffusion MRI, dynamic contrast MRI and proton MR spectroscopy[35–37] will improve characterization of the salivary tumours.

Conclusion

We concluded that combined FA and MD can differentiate malignant from benign salivary gland tumours, differentiate Warthin tumours from pleomorphic adenomas and malignant tumours from pleomorphic adenomas and FA can differentiate Warthin tumours from malignancy.

REFERENCES

1. Del Signore AG, Megwalu UC. The rising incidence of major salivary gland cancer in the United States. *Ear Nose Throat J* 2017; **96**: E13–E16.
2. Carlson ER. Management of parotid tumors. *J Oral Maxillofac Surg* 2017; **75**: 247–8. doi: https://doi.org/10.1016/j.joms.2016.12.001
3. Freling N, Crippa F, Maroldi R. Staging and follow-up of high-grade malignant salivary gland tumours: the role of traditional versus functional imaging approaches - a review. *Oral Oncol* 2016; **60**: 157–66. doi: https://doi.org/10.1016/j.oraloncology.2016.04.016
4. Abdel Razek AA, Ashmalla GA, Gaballa G, Nada N. Pilot study of ultrasound parotid imaging reporting and data system (PIRADS): inter-observer agreement. *Eur J Radiol* 2015; **84**: 2533–8. doi: https://doi.org/10.1016/j.ejrad.2015.09.001
5. Mansour N, Hofauer B, Knopf A. Ultrasound elastography in diffuse and focal parotid gland lesions. *ORL J Otorhinolaryngol Relat Spec* 2017; **79**: 54–64. doi: https://doi.org/10.1159/000455727
6. Dong Y, Lei GW, Wang SW, Zheng SW, Ge Y, Wei FC. Diagnostic value of CT perfusion imaging for parotid neoplasms. *Dentomaxillofac Radiol* 2014; **43**: 20130237. doi: https://doi.org/10.1259/dmfr.20130237
7. Razek AA, Tawfik AM, Elsorogy LG, Soliman NY. Perfusion CT of head and neck cancer. *Eur J Radiol* 2014; **83**: 537–44. doi: https://doi.org/10.1016/j.ejrad.2013.12.008
8. Chawla A, Srinivasan S, Lim TC, Pulickal GG, Shenoy J, Peh WCG. Dual-energy CT applications in salivary gland lesions. *Br J Radiol* 2017; **90**: 20160859. doi: https://doi.org/10.1259/bjr.20160859
9. Prasad RS. Parotid gland imaging. *Otolaryngol Clin North Am* 2016; **49**: 285–312. doi: https://doi.org/10.1016/j.otc.2015.10.003
10. Kuan EC, Mallen-St Clair J, St John MA. Evaluation of parotid lesions. *Otolaryngol Clin North Am* 2016; **49**: 313–25. doi: https://doi.org/10.1016/j.otc.2015.10.004
11. Abdel Razek A, Mukherji S. State of art imaging of salivary gland tumors. *Neuroimag Clin North Am* 2018; **27**.
12. Christe A, Waldherr C, Hallett R, Zbaeren P, Thoeny H. MR imaging of parotid tumors: typical lesion characteristics in MR imaging improve discrimination between benign and malignant disease. *AJNR Am J Neuroradiol* 2011; **32**: 1202–7. doi: https://doi.org/10.3174/ajnr.A2520
13. Thoeny HC, De Keyzer F, King AD. Diffusion-weighted MR imaging in the head and neck. *Radiology* 2012; **263**: 19–32. doi: https://doi.org/10.1148/radiol.11101821
14. Milad P, Elbegiermy M, Shokry T, Mahmoud H, Kamal I, Taha MS, et al. The added value of pretreatment DW MRI in characterization of salivary glands pathologies. *Am J Otolaryngol* 2017; **38**: 13–20. doi: https://doi.org/10.1016/j.amjoto.2016.09.002
15. Razek AAKA. Prediction of malignancy of submandibular gland tumors with apparent diffusion coefficient. *Oral Radiol* 2017; **39**. doi: https://doi.org/10.1007/s11282-017-0311-y
16. Lam PD, Kuribayashi A, Imaizumi A, Sakamoto J, Sumi Y, Yoshino N, et al. Differentiating benign and malignant salivary gland tumours: diagnostic criteria and the accuracy of dynamic contrast-enhanced MRI with high temporal resolution. *Br J Radiol* 2015; **88**: 20140685. doi: https://doi.org/10.1259/bjr.20140685
17. Abdel Razek AA, Samir S, Ashmalla GA. Characterization of parotid tumors with dynamic susceptibility contrast perfusion-weighted magnetic resonance imaging and diffusion-weighted MR imaging. *J Comput Assist Tomogr* 2017; **41**: 131–6. doi: https://doi.org/10.1097/RCT.0000000000000486
18. Kato H, Kanematsu M, Watanabe H, Kajita K, Mizuta K, Aoki M, et al. Perfusion imaging of parotid gland tumours: usefulness of arterial spin labeling for differentiating Warthin's tumours. *Eur Radiol* 2015; **25**: 3247–54. doi: https://doi.org/10.1007/s00330-015-3755-7
19. Tao X, Yang G, Wang P, Wu Y, Zhu W, Shi H, et al. The value of combining conventional, diffusion-weighted and dynamic contrast-enhanced MR imaging for the diagnosis of parotid gland tumours. *Dentomaxillofac Radiol* 2017; **46**: 20160434. doi: https://doi.org/10.1259/dmfr.20160434

20. Alexander DC, Dyrby TB, Nilsson M, Zhang H. Imaging brain microstructure with diffusion MRI: practicality and applications. *NMR Biomed* 2017: e3841. doi: https://doi.org/10.1002/nbm.3841
21. Abdel Razek AA, Nada N. Role of diffusion-weighted MRI in differentiation of masticator space malignancy from infection. *Dentomaxillofac Radiol* 2013; **42**: 20120183. doi: https://doi.org/10.1259/dmfr.20120183
22. Razek AA, Sieza S, Maha B. Assessment of nasal and paranasal sinus masses by diffusion-weighted MR imaging. *J Neuroradiol* 2009; **36**: 206–11. doi: https://doi.org/10.1016/j.neurad.2009.06.001
23. Potgieser AR, Wagemakers M, van Hulzen AL, de Jong BM, Hoving EW, Groen RJ. The role of diffusion tensor imaging in brain tumor surgery: a review of the literature. *Clin Neurol Neurosurg* 2014; **124**: 51–8. doi: https://doi.org/10.1016/j.clineuro.2014.06.009
24. Takumi K, Fukukura Y, Hakamada H, Ideue J, Kumagae Y, Yoshiura T. Value of diffusion tensor imaging in differentiating malignant from benign parotid gland tumors. *Eur J Radiol* 2017; **95**: 249–56. doi: https://doi.org/10.1016/j.ejrad.2017.08.013
25. Koontz NA, Wiggins RH. Differentiation of benign and malignant head and neck lesions with diffusion tensor imaging and DWI. *AJR Am J Roentgenol* 2017; **208**: 1110–5. doi: https://doi.org/10.2214/AJR.16.16486
26. Yu J, Du Y, Lu Y, Zhang W, Zhang D, Wang G, et al. Application of DTI and ARFI imaging in differential diagnosis of parotid tumours. *Dentomaxillofac Radiol* 2016; **45**: 20160100. doi: https://doi.org/10.1259/dmfr.20160100
27. Razek A, El-Serougy L, Abdelsalam M, Gaballa G, Talaat M. Differentiation of residual/recurrent gliomas from postradiation necrosis with arterial spin labeling and diffusion tensor magnetic resonance imaging-derived metrics. *Neuroradiology* 2018; **60**: 169–77. doi: https://doi.org/10.1007/s00234-017-1955-3
28. El-Serougy L, Abdel Razek AA, Ezzat A, Eldawoody H, El-Morsy A. Assessment of diffusion tensor imaging metrics in differentiating low-grade from high-grade gliomas. *Neuroradiol J* 2016; **29**: 400–7. doi: https://doi.org/10.1177/1971400916665382
29. Razek A, Shabana AAE, El Saied TO, Alrefey N. Diffusion tensor imaging of mild-moderate carpal tunnel syndrome: correlation with nerve conduction study and clinical tests. *Clin Rheumatol* 2017; **36**: 2319–24. doi: https://doi.org/10.1007/s10067-016-3463-y
30. Mikaszewski B, Markiet K, Smugała A, Stodulski D, Szurowska E, Stankiewicz C. Diffusion-weighted MRI in the differential diagnosis of parotid malignancies and pleomorphic adenomas: can the accuracy of dynamic MRI be enhanced? *Oral Surg Oral Med Oral Pathol Oral Radiol* 2017; **124**: 95–103. doi: https://doi.org/10.1016/j.oooo.2017.03.007
31. Espinoza S, Felter A, Malinvaud D, Badoual C, Chatellier G, Siauve N, et al. Warthin's tumor of parotid gland: surgery or follow-up? Diagnostic value of a decisional algorithm with functional MRI. *Diagn Interv Imaging* 2016; **97**: 37–43. doi: https://doi.org/10.1016/j.diii.2014.11.024
32. Miao LY, Xue H, Ge HY, Wang JR, Jia JW, Cui LG. Differentiation of pleomorphic adenoma and Warthin's tumour of the salivary gland: is long-to-short diameter ratio a useful parameter? *Clin Radiol* 2015; **70**: 1212–9. doi: https://doi.org/10.1016/j.crad.2015.06.085
33. Fujima N, Sakashita T, Homma A, Shimizu Y, Yoshida A, Harada T, et al. Advanced diffusion models in head and neck squamous cell carcinoma patients: goodness of fit, relationships among diffusion parameters and comparison with dynamic contrast-enhanced perfusion. *Magn Reson Imaging* 2017; **36**: 16–23. doi: https://doi.org/10.1016/j.mri.2016.10.024
34. Kim HS, Goh MJ, Kim N, Choi CG, Kim SJ, Kim JH. Which combination of MR imaging modalities is best for predicting recurrent glioblastoma? Study of diagnostic accuracy and reproducibility. *Radiology* 2014; **273**: 831–43. doi: https://doi.org/10.1148/radiol.14132868
35. Abdel Razek A. Routine and advanced Diffusion imaging modules of the salivary glands. *Neuroimag Clin North Am* 2018; **27**.
36. Abdel Razek AA, Gaballa G. Role of perfusion magnetic resonance imaging in cervical lymphadenopathy. *J Comput Assist Tomogr* 2011; **35**: 21–5. doi: https://doi.org/10.1097/RCT.0b013e3181ff9143
37. Razek AA, Nada N. Correlation of choline/creatine and apparent diffusion coefficient values with the prognostic parameters of head and neck squamous cell carcinoma. *NMR Biomed* 2016; **29**: 483–9. doi: https://doi.org/10.1002/nbm.3472